Spectroscopic Characterization of a High-Affinity Calmodulin−Target Peptide Hybrid Molecule†

Stephen R. Martin,‡ Peter M. Bayley,*,‡ Susan E. Brown,‡,§ Tudor Porumb,|| Mingjie Zhang,||,⊥ and Mitsuhiko Ikura||

Division of Physical Biochemistry, National Institute for Medical Research, Mill Hill, London NW7 1AA, U.K., and Division of Molecular and Structural Biology, Ontario Cancer Institute, and Department of Medical Biophysics, University of Toronto, 610 University Avenue, Toronto, Ontario, Canada M5G 2M9

Received October 23, 1995; Revised Manuscript Received December 21, 1995⊗

ABSTRACT: We describe the properties of a hybrid protein comprising the full length of the *Xenopus laevis* calmodulin sequence, followed by a pentapeptide linker (GGGGS), and residues 3−26 of M13, the calmodulin binding region of skeletal muscle myosin light chain kinase. The properties of the hybrid protein are compared with those of the complex formed between *Drosophila* calmodulin and a peptide corresponding to residues 1−18 of the M13 sequence. The addition of calcium to the hybrid protein produces pronounced changes in the near- and far-UV CD spectra, in the fluorescence emission spectrum of the single tryptophan residue at position 4 in the M13 sequence, and in the accessibility of this tryptophan residue to acrylamide quenching. These changes are consistent with the tryptophan residue being immobilized in a hydrophobic environment and with the hybrid protein adopting a more α-helical structure when calcium is bound. The increased α-helicity derives from changes in both the calmodulin and peptide regions of the hybrid protein. Changes in the circular dichroism and fluorescence properties of the hybrid protein as a function of the calcium to hybrid protein ratio are consistent with the fact that these changes parallel the cooperative binding of all four calcium ions. The hybrid protein shows greatly increased affinity (>250-fold) for calcium compared with calmodulin itself. Macroscopic calcium binding constants (K_1−K_4) were determined from calcium titrations performed in the presence of the calcium chelator Quin 2. Values for $\log(K_1K_2)$ and $\log(K_3K_4)$ were determined to be 15.4 ± 0.2 and 15.59 ± 0.22 (20 °C). The corresponding values for *Drosophila* calmodulin alone are 11.65 ± 0.15 and 9.66 ± 0.25. Consistent with this increased affinity for calcium, stopped-flow kinetic studies suggest that the dissociation rate for the N-terminal calcium ions is reduced to at least 0.77 s^{-1}, compared with ≈700 s^{-1} for *Drosophila* calmodulin in the absence of peptide. This hybrid protein illustrates the principle whereby the binding of a peptide sequence covalently attached to calmodulin can enhance the average calcium affinity by more than 2 orders of magnitude. Conversely, the target sequence in the hybrid protein undergoes a calcium-induced conformational change to bind to the calmodulin in a conformation very similar to that of the corresponding dissociable target sequence binding to calmodulin, but with a greatly enhanced affinity due to its physical proximity to the binding site. This avoidance of the energetic penalty of dissociation may be a key contributory factor in determining the high affinity and specificity of the complex multiple interactions involved in recognition of biological targets by calmodulin.

Downloaded via HONG KONG UNIV SCIENCE TECHLGY on August 7, 2019 at 14:05:48 (UTC).
See https://pubs.acs.org/sharingguidelines for options on how to legitimately share published articles.

Calmodulin is a eukaryotic calcium binding protein which regulates the activity of a large number of target proteins (Davis, 1992). Calmodulin consists of two structurally similar globular domains each containing a pair of helix−loop−helix (EF-hand) calcium binding sites. In the crystal structure, the two globular domains are separated by a long central α-helix to produce a dumbbell-like structure (Babu et al., 1988). However, NMR studies show that the middle section of the central helix (residues 77−81) is disrupted in solution and acts as a flexible linker between the two semirigid domains of both Ca_4-CaM (Barbato et al., 1992) and apo-CaM (Zhang et al., 1995; Kuboniwa et al., 1995).

The solution structure of a complex of calcium-saturated calmodulin (Ca_4-CaM) and a 26-residue peptide (M13) corresponding to the calmodulin binding site of skeletal muscle myosin light chain kinase (sk-MLCK) has been solved by multidimensional NMR (Ikura et al., 1992). The two globular domains retain their overall shape, but they enclose the peptide sequence. The linker region between the domains consists of two short helices connected by a flexible loop running from residues 74−81 (Ikura et al., 1992). The crystal structure of a complex of Ca_4-CaM and a peptide from smooth muscle myosin light chain kinase has also been determined (Meador et al., 1992). The crystal structure is very similar to the solution structure of Ca_4-CaM−M13 except that in the crystal structure the bend in

† This work was supported in part by the Medical Research Council of Canada (to M.I.). S.E.B. gratefully acknowledges the support of the George Murray Fellowship from the University of Adelaide, Australia.

* Address correspondence to this author at the Division of Physical Biochemistry, National Institute for Medical Research, The Ridgeway, Mill Hill, London NW7 1AA, U.K. Phone: 0181-959-3666. Fax: 0181-906-4477.

‡ National Institute for Medical Research.

§ Present address: Department of Biochemistry and Molecular Biology, University of British Columbia, 2146 Health Sciences Mall, Vancouver, British Columbia, Canada V6T 1Z3.

|| Ontario Cancer Institute and University of Toronto.

⊥ Present address: Department of Biochemistry, Hong Kong University of Science and Technology, Clear Water Bay, Kowloon, Hong Kong.

⊗ Abstract published in *Advance ACS Abstracts,* March 1, 1996.

0006-2960/96/0435-3508$12.00/0 © 1996 American Chemical Society

the central helix is well-defined and occurs between residues 73 and 77. M13 and related peptides have little regular secondary structure when free in aqueous solution but become helical when complexed with Ca_4-CaM (Ikura et al., 1992; Findlay et al., 1995a).

The calcium binding properties of calmodulin have been studied by many groups and have been reviewed by Forsén et al. (1986). The binding of the two calcium ions within an individual domain shows positive cooperativity, but there is no detectable interdomain cooperativity (Linse et al., 1991a). Calcium binding sites I and II in the N-terminal domain have lower affinity for calcium than sites III and IV in the C-terminal domain (Thulin et al., 1984; Martin et al., 1985). Reported pCa(50%) values are generally in the range 5.1−5.7 for measurements performed in the presence of 100 mM KCl.

The apparent affinity of calmodulin for calcium is greatly increased by the addition of target proteins and peptides. This has been shown by calcium binding studies performed in the presence of myosin light chain kinase (Olwin & Storm, 1985), cyclic nucleotide phosphodiesterase (Olwin & Storm, 1985), caldesmon (Yazawa et al., 1987), melittin (Maulet & Cox, 1983), mastoparan (Yazawa et al., 1987), the M13 peptide from skeletal myosin light chain kinase (Yagi et al., 1989), and a synthetic peptide derived from the plasma membrane Ca^{2+} pump (Yazawa et al., 1992). In the latter case, the presence of the peptide increases the affinity of calcium so that pCa(50%) is increased from 5.22 to 7.42 (Yazawa et al., 1992). This also means that the affinity of the peptide for calmodulin is increased by a factor of 6.2×10^8 by the presence of calcium (Yazawa et al., 1992). Similar increases in affinity are observed for many calmodulin binding peptides. The affinities of peptides for calmodulin in the absence of calcium are generally low and are not easily measured. In the presence of target proteins and peptides, calcium binding sometimes appears to be cooperative between all four binding sites (Yazawa et al., 1987; Ikura et al., 1989), though this is apparently not always the case (Yazawa et al., 1992).

In the Ca_4-CaM−M13 complex, the C-terminus of the calmodulin and the N-terminus of the peptide are in close proximity (Ikura et al., 1992). This suggested the possibility of linking the N-terminus of the 26-residue M13 peptide to the C-terminus of calmodulin, and Porumb et al. (1994) described the properties of a hybrid protein comprising the full length of the *Xenopus laevis* calmodulin sequence, followed through a glycylglycine linker, by the 26 residues of M13. NMR studies (Porumb et al., 1994) showed that the hybrid protein existed in solution as a mixture (approximately 1:1) of two major conformations, one similar to the compact globular structure of the Ca_4-CaM−M13 complex (Ikura et al., 1992) and the other similar to the dumbbell-like structure of the wild-type calmodulin (Babu et al., 1988).

Here, we describe the properties of a new hybrid protein comprising the full length of the *Xenopus laevis* calmodulin sequence, followed through a pentapeptide linker (GGGGS), by residues 3−26 of M13. We compare this hybrid protein with the complex formed between *Drosophila* calmodulin and the peptide WFF corresponding to residues 1−18 of M13. We assess the conformational properties of the hybrid complex formed in the presence of Ca^{2+}, and quantify the enhancement of affinity of Ca^{2+} due to the presence of the covalently attached peptide.

MATERIALS AND METHODS

Construction of the pHY2 Expression Vector. pHY2 is a derivative of pHY1 which is designed to express a calmodulin−M13 hybrid (Porumb et al., 1994). The Gly-Gly linker and the first two residues (Lys-Arg) of the M13 peptide in the first hybrid were replaced with Gly-Gly-Gly-Gly-Ser. This was achieved by site-directed mutagenesis using the overlap extension method described by Ho et al. (1989). The polymerase chain reaction product was subsequently subcloned into pHY1, yielding a new hybrid-expressing vector, pHY2.

Proteins and Peptides. The H2CaM hybrid gene was expressed in *E. coli* following the procedure described for the first CaM−target peptide gene (Porumb et al., 1994). The hybrid protein was prepared using the purification system described by Porumb et al. (1994), with the exception that EGTA was used as chelator instead of DTPA during the decalcification by trichloroacetic acid precipitation and renaturation steps. *Drosophila melanogaster* calmodulin (CaM) expressed in *E. coli* was purified as described by Findlay et al. (1995a). The purified proteins ran as single bands on SDS−PAGE (15% gel, Laemmli system). The WFF peptide (KKRWKKNFIAVSAANRFK, residues 1−18 of the M13 sequence) with free amino and carboxy termini was synthesized on an Applied Biosystems 430A peptide synthesizer and purified by HPLC on a C18 column. All concentrations were determined spectrophotometrically using the following extinction coefficients: 5690 M^{-1} cm^{-1} at 280 nm for the WFF peptide [calculated for one Trp (Gill & von Hippel, 1989)]; 1578 M^{-1} cm^{-1} at 279 nm for *Drosophila* calmodulin in the presence of excess calcium (Maune et al., 1992b); 8250 M^{-1} cm^{-1} at 280 nm for the hybrid protein [calculated for one Trp and two Tyr (Gill & von Hippel, 1989)]. *Drosophila* calmodulin was made calcium-free by incubating with 5 mM EGTA and then desalting by passage though two Pharmacia PD10 (G25) columns equilibrated with 25 mM Tris, 100 mM KCl, pH 8.0. For the NMR experiments, the protein concentration was ≈1 mM, and the residual Ca^{2+} level, determined by atomic absorption spectroscopy, was less than 0.1 ($[Ca^{2+}]$/[H2CaM])

Fluorescence Measurements. Uncorrected tryptophan fluorescence emission spectra were recorded using a SPEX FluoroMax fluorimeter with excitation at 290 nm (bandwidth 1.7 nm) and emission scanned from 300 to 400 nm (bandwidth 5 nm). Spectra were recorded at 20 °C in UV-transmitting plastic cuvettes. The buffer was 25 mM Tris, 100 mM KCl, pH 8.0, unless otherwise noted, and protein/peptide concentrations were in the range 1−2.5 μM. Acrylamide quenching studies were performed by adding small aliquots of concentrated acrylamide to protein/peptide solutions containing either 1 mM calcium or 1 mM EGTA and monitoring the fluorescence emission at 340 nm (for Ca_4-H2CaM and Ca_4-CaM−WFF), 345 nm (for apo-H2CaM), and 355 nm (for free WFF peptide). The results were analyzed using the modified Stern−Volmer equation (Eftink & Ghiron, 1976):

$$F_0/F = (1 + K_{SV}[Q])e^{V[Q]}$$

where F_0 and F are the fluorescence in the absence and presence of acrylamide, respectively, [Q] is the concentration of acrylamide, K_{SV} is the Stern−Volmer constant for collisional quenching, and V is the static quenching constant. The values reported for K_{SV} and V are the averages of values obtained from at least three separate titrations.

Circular Dichroism Measurements. CD spectra were recorded on a Jasco J-600 spectropolarimeter at 20 °C in 25 mM Tris, 100 mM KCl at pH 8.0. Far-UV CD spectra (190−260 nm) were measured using 1 or 2 mm fused silica cuvettes with peptide/protein concentrations in the range 4−10 μM. Near-UV CD spectra (250−340 nm) were measured using 10 mm fused silica cuvettes with peptide/protein concentrations in the range 40−60 μM. Multiple scans were averaged ($\geq$8 for near-UV and $\geq$4 for far-UV), base lines were subtracted, and a small degree of numerical smoothing was applied. Spectra are presented as the circular dichroism absorption coefficient calculated using the molar concentration of peptide or protein ($=\Delta\epsilon_M$), rather than on a per residue basis, in order to facilitate direct comparison of free proteins, peptides, and protein−peptide complexes. Values of $\Delta\epsilon_{MRW}$ can be obtained by dividing $\Delta\epsilon_M$ by the appropriate number of peptide bonds.

NMR Measurements. $^1H-^{15}N$ HSQC spectra were recorded at 37 °C on a Varian Unity-plus 500 MHz spectrometer equipped with a triple-resonance, pulse field gradient probe with an actively shielded z gradient and a gradient amplifier unit, using the pulse scheme described elsewhere (Kay et al., 1992). Except for the Ca^{2+} titration studies where 128 experiments were acquired in F_1, a total of 256 experiments (16 scans in each experiment) with 1024 complex points in F_2 were collected for each $^1H-^{15}N$ HSQC experiment. The data were processed using the software nmrPipe and nmrDraw written by F. Delgagio at NIH. A Lorentzian−Gaussian apodization function was used for the F_2 dimension, and a 63°-shifted sine-square window function was applied in F_1.

Stopped-Flow Measurements. Kinetic measurements were performed with a Hi-Tech SF61-MX stopped-flow spectrophotometer. The excitation monochromator was set to 290 nm (band-pass = 5 nm), and tryptophan emission was detected using a 320 nm cuton filter. The measurements were made in 25 mM Tris, 100 mM KCl, pH 8.0, buffer at 20 °C unless otherwise noted. The concentrations quoted are those prior to stopped-flow mixing, and the rate constants are the averages of at least nine traces.

Calcium Binding Studies. Macroscopic calcium binding constants (K_1-K_4) were determined from calcium titrations performed in the presence of the chromophoric calcium chelators, 5,5′-Br_2BAPTA (for CaM alone) or Quin 2 (for CaM plus WFF peptide and for H2CaM), using the method described by Linse et al. (1988, 1991a) and Waltersson et al. (1993). Measurements were performed at 20 °C in 10 mM Tris, 100 mM KCl, pH 8; under these conditions, we have determined the calcium binding constants of 5,5′-Br_2-BAPTA and Quin 2 to be 5.7×10^5 M^{-1} and 1.1×10^7 M^{-1} [cf. values of 6.3×10^5 M^{-1} and 1.2×10^7 M^{-1}, respectively, reported by Linse et al. (1991b) under similar conditions]. At least three separate titrations were performed on each protein sample, and the values for the individual binding constants (K_1-K_4) were obtained from least-squares fits directly to the experimentally observed titration curves (Linse et al., 1991a). As noted by Linse et al. (1991a) and Porumb (1994), the values of $\log(K_1K_2)$ and $\log(K_3K_4)$ are better determined than individual $\log(K_i)$ values.

RESULTS

NMR Studies. Unlike the similar hybrid protein described in an earlier report (Porumb et al., 1994), the new M13/CaM hybrid protein with the GGGGS pentapeptide linker (H2CaM) exists as a single conformer in solution. Figure 1A shows a portion of the $^1H-^{15}N$ HSQC spectrum of Ca_4-H2CaM uniformly labeled with ^{15}N. The data clearly indicate that each backbone amide gives rise to a single peak in the spectrum. Moreover, the $^1H-^{15}N$ HSQC spectrum of Ca_4-H2CaM is remarkably similar to that of the Ca_4-CaM−M13 complex (Figure 1B), except that some new peaks which correspond to the amides from the M13 peptide were also observed in the spectrum of Ca_4-H2CaM (peaks labeled with an asterisk in Figure 1A). The results strongly suggest that the solution structure of Ca_4-H2CaM is very similar to that of Ca_4-CaM−M13 (Ikura et al., 1992).

Fluorescence Studies. Upon binding to Ca_4-CaM, the fluorescence emission maximum of the Trp-4 in the WFF peptide shifts from 356 to 334 nm, and the emission intensity increases, as shown in Figure 2A. This signal intensification and blue-shift in the emission maximum are consistent with the Trp-4 being in a more hydrophobic environment when the peptide is bound to the calmodulin (Findlay et al., 1995a). The addition of excess EGTA to the Ca_4-CaM−WFF complex produces the emission spectrum of the free WFF peptide, confirming that there is no interaction between peptide and protein in the absence of calcium under these buffer conditions [cf. Kilhoffer et al. (1992)]. The fluorescence emission properties of Ca_4-H2CaM are similar to those of Ca_4-CaM−WFF, except that the emission maximum is at 332 nm. However, the emission properties of apo-H2CaM differ significantly from those of the free WFF peptide, which are typical for a short tryptophan-containing peptide. The emission maximum is 344 nm (compared with 356 nm for the free WFF peptide), and the emission intensity is significantly greater. Both these observations suggest that the Trp residue in the hybrid protein is only partially exposed to solvent in the absence of calcium. The emission properties of apo-H2CaM are largely unaffected by changes in temperature in the range 5−35 °C (other than the normal effect of temperature on fluorescence), suggesting that the observed emission properties derive from a single conformation of apo-H2CaM. The addition of 3 M urea to apo-H2CAM has little effect on the emission properties; however, the addition of high concentrations of KCl (up to 0.7 M) produces a small shift in the emission maximum (to 349 nm) and a reduction in the emission intensity (data not shown).

Acrylamide quenching studies were performed in order to investigate further the question of solvent accessibility. The results are shown in Figure 2B. The pattern of quenching behavior for Ca_4-H2CaM ($K_{SV} = 0.59 \pm 0.2$ M^{-1} and $V = 0.25 \pm 0.1$ M^{-1}) is very similar to that for the Ca_4-CaM−WFF complex ($K_{SV} = 0.65 \pm 0.2$ M^{-1} and $V = 0.3 \pm 0.1$ M^{-1}). For free WFF peptide, we find $K_{SV} = 21.0 \pm 3.0$ M^{-1} and $V = 1.0 \pm 0.5$ M^{-1}; the latter values are, as expected, typical for completely exposed tryptophan (Eftink & Ghiron, 1976). However, for apo-H2CaM we find $K_{SV} = 3.2 \pm 0.5$ M^{-1} and $V = 0.6 \pm 0.2$ M^{-1}. These values support the view that the tryptophan residue is only partially solvent-exposed in apo-H2CaM.

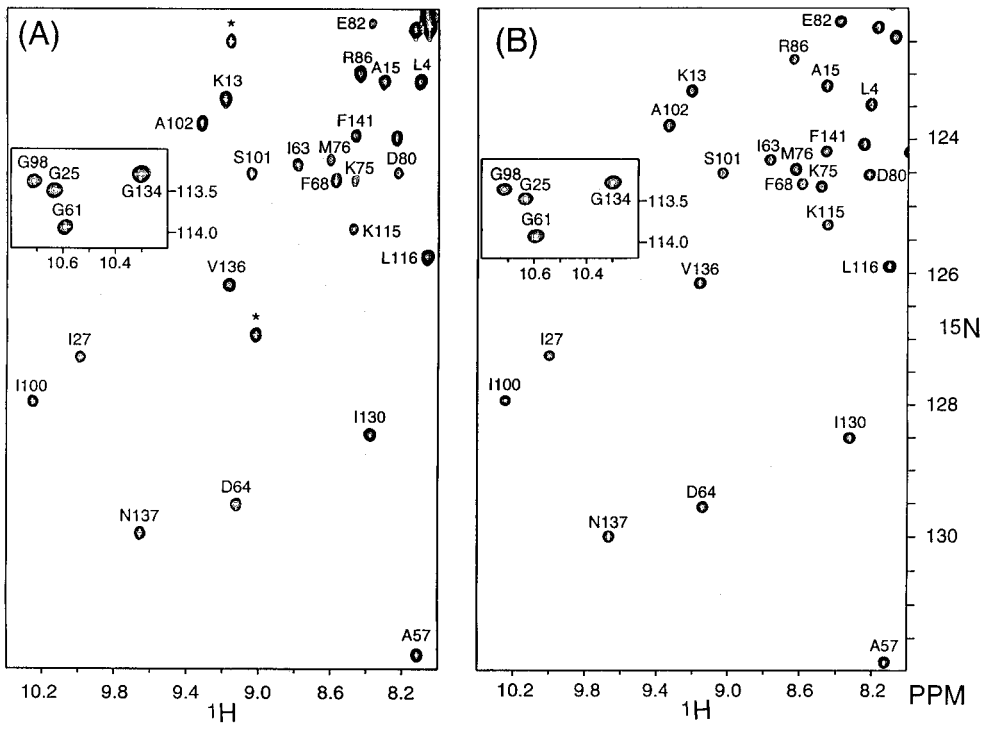

FIGURE 1: Portion of the $^1H-^{15}N$ HSQC spectrum of (A) ^{15}N-uniformly-labeled H2CaM and (B) ^{15}N-uniformly-labeled Ca_4-CaM complex with the M13 peptide. For clarity, well-resolved regions which include resonances from Ca^{2+} binding sites, helical parts, and unstructured regions of the protein were selected to show that the two spectra are very similar. The resonances labeled with an asterisk in (A) represent the amides from the M13 peptide. The spectra were recorded at pH 6.8, 37 °C, in an H_2O/D_2O (90/10 vol %). The sample concentration was ≈1.5 mM in both cases.

Changes in the fluorescence emission intensity as a function of added calcium are shown in Figure 2C. For the hybrid protein, the major change in tryptophan fluorescence occurs as the [calcium]/[CaM] ratio ($=R_{Ca}$) changes from (approximately) 1 to 3. In contrast, for CaM plus WFF peptide, the major fluorescence change occurs as R_{Ca} changes from 0 to 2.

Near-UV Circular Dichroism. Figure 3A shows the near-UV (or aromatic, 320−255 nm) CD spectrum of a 1:1 mixture of apo-CaM and WFF peptide (curve a). This is closely similar to the spectrum of apo-CaM previously reported by Maune et al. (1992a), which supports the finding from the fluorescence measurements that CaM does not interact with the WFF peptide in the absence of calcium in these buffer conditions. The addition of excess calcium produces major spectral changes throughout the near-UV region (curve b). These changes derive from two effects. The appearance of the long-wavelength maximum (295 nm) is associated with the immobilization of Trp-4 of the peptide on formation of the Ca_4-CaM−WFF complex (Findlay et al., 1995a), while the changes at lower wavelengths presumably derive, at least in part, from changes in the environment of Tyr-138 and some phenylalanine residues in the calmodulin induced by calcium binding (Maune et al., 1992a). These conclusions are supported by the following arguments. The CD difference spectrum [Ca_4-CaM−WFF complex minus Ca_4-CaM minus free WFF peptide] produces the spectrum of bound WFF (curve c). Note that curve c has the long-wavelength maximum but has rather low intensity at shorter wavelengths. The CD difference spectrum [Ca_4-CaM minus apo-CaM] gives the effect of calcium on the tyrosine and phenylalanine residues in calmodulin (curve d in Figure 3A). The summation of curves a, c, and d is then shown as the dotted line and is seen to be closely similar to curve b.

Figure 3B (curve a) shows the near-UV CD spectrum of apo-H2CaM. This is similar to the spectrum of calcium-free porcine brain CaM previously reported by Török et al. (1992). Note that the porcine and *Xenopus* proteins have tyrosine residues in positions 99 and 138, whereas the *Drosophila* protein lacks Tyr-99. The addition of excess calcium again produces major spectral changes throughout the near-UV region (curve b). By analogy with the results for calmodulin plus WFF peptide, we assume that the new long-wavelength maximum (295 nm) is associated with the immobilization of the tryptophan brought about by calcium binding, while the changes at lower wavelengths derive from calcium-induced changes in the environments of Tyr-99, Tyr-138, and some phenylalanine residues in the calmodulin (see above).

Changes in CD intensity as a function of added calcium are shown in Figure 3C for 295 nm (Trp-4 in the peptide) and 278 nm (tyrosines in the calmodulin). For CaM plus WFF peptide, the changes occur in parallel and saturate at R_{Ca} (=[calcium]/[CaM]) slightly greater than 2. The saturation behavior for the tyrosine signal suggests that in the presence of the WFF peptide the first two calcium ions added bind preferentially to sites III and IV in the tyrosine-containing C-terminal domain of the calmodulin. Similar behavior is observed when the experiment is performed in the absence of added peptides (Maune et al., 1992a). The appearance of the WFF peptide tryptophan signal (295 nm) in parallel with the calmodulin tyrosine signal (278 nm) shows that the peptide is able to bind to calmodulin species with only sites III and IV occupied by calcium. No further spectroscopic changes occur as sites I and II become

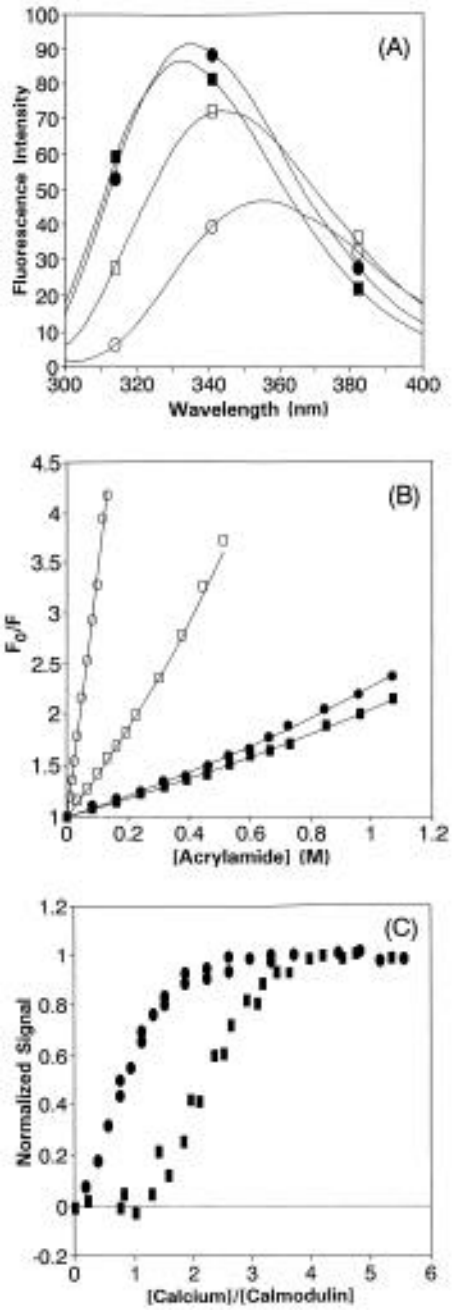

FIGURE 2: (A) Tryptophan fluorescence emission spectra (λ_{ex} = 290 nm) of free WFF peptide (○), Ca_4-CaM−WFF (●), apo-H2CaM (□), and Ca_4-H2CaM (■). Peptide and protein concentrations were 2.5 μM, and spectra were recorded at 20 °C in 25 mM Tris, 100 mM KCl, pH 8. (B) Stern−Volmer plots for acrylamide quenching of free WFF peptide (○), Ca_4-CaM−WFF (●), apo-H2CaM (□), and Ca_4-H2CaM (■). Peptide and protein concentrations were 2.5 μM, and spectra were recorded at 20 °C in 25 mM Tris, 100 mM KCl, pH 8. (C) Fractional change in fluorescence emission intensity at 330 nm (λ_{ex} = 290 nm) as a function of R_{Ca} (=[calcium]/[CaM]) for the hybrid protein (■) and for calmodulin plus WFF peptide (●). The measurements were made at 20 °C in 25 mM Tris, 100 mM KCl, pH 8. Two separate experiments are shown for each protein.

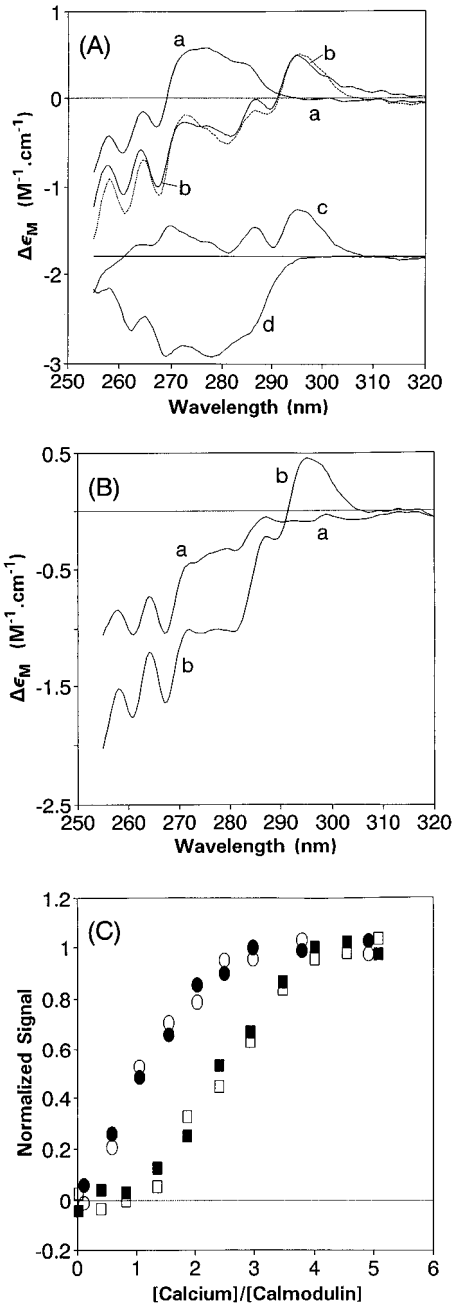

FIGURE 3: (A) Near-UV circular dichroism spectra of calmodulin plus WFF peptide in the absence (a) and presence (b) of calcium. Curve c shows the calculated difference spectrum, Ca_4-CaM−WFF minus Ca_4-CaM minus free WFF peptide. Curve d shows the calculated difference spectrum, Ca_4-CaM minus apo-CaM. The dotted line shows the summation of curves a, c, and d. The measurements were made at 20 °C in 25 mM Tris, 100 mM KCl, pH 8. (B) Near-UV circular dichroism spectra of the hybrid protein in the absence (a) and presence (b) of calcium. The measurements were made at 20 °C in 25 mM Tris, 100 mM KCl, pH 8. (C) Fractional change in circular dichroism signals at 278 (calmodulin tyrosine signal) and 295 nm (peptide tryptophan signal) as a function of R_{Ca} (=[calcium]/[CaM]) for the hybrid protein (□, 278 nm; ■, 295 nm) and for calmodulin plus WFF peptide (○, 278 nm; ●, 295 nm). The measurements were made at 20 °C in 25 mM Tris, 100 mM KCl, pH 8.

occupied. For the hybrid protein, the changes at 278 and 295 nm also occur in parallel, but the dependence upon R_{Ca} is very different. There is little spectroscopic change associated with either tyrosine or tryptophan chromophores for $R_{Ca} < 1$; then the bulk of the change occurs for R_{Ca} values between 1.5 and 3.5, and the changes are complete as R_{Ca} approaches 4.

Far-UV Circular Dichroism. It is well established that calmodulin shows a marked increase in intensity of peptide CD on addition of calcium, and this is usually interpreted as due to an increase in the amount of α-helical structure (e.g., Martin & Bayley, 1986). Recent NMR work (Finn et al., 1995; Kubinowa et al., 1995; Zhang et al., 1995) has

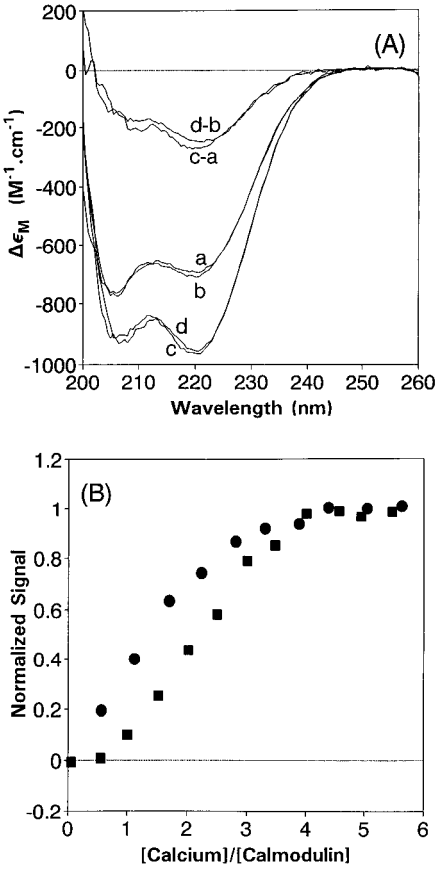

FIGURE 4: (A) Far-UV circular dichroism spectra of calmodulin plus WFF peptide in the absence (a) and presence of excess calcium (c), and of the hybrid protein in the absence (b) and presence (d) of excess calcium. The appropriate difference spectra are labeled as c−a for calmodulin plus WFF peptide and d−b for the hybrid protein. Spectra were recorded at 20 °C in 25 mM Tris, 100 mM KCl, pH 8. (B) Fractional change in the circular dichroism signal at 220 nm as a function of R_{Ca} (=[calcium]/[CaM]) for the hybrid protein (■) and for calmodulin plus WFF peptide (●). The measurements were made at 20 °C in 25 mM Tris, 100 mM KCl, pH 8.

shown that the helical elements of holo-calmodulin can be identified as being present also in apo-calmodulin, although the fraction of secondary structure in the full population is not precisely quantitated. Compared to holo-calmodulin, apo-calmodulin has a high degree of dynamics, particularly in the C-domain which shows some conformational equilibrium (Tjandra et al., 1995) and is sensitive to ionic conditions (Urbauer et al., 1995). Thus, the CD and NMR techniques (depending on the precise details of the experiment) may report on somewhat different fractions of a dynamic population of apo-calmodulin molecules.

Figure 4A shows the far-UV (260−200 nm) CD spectrum of a 1:1 mixture of apo-CaM and WFF peptide (curve a). This is similar to the spectrum of apo-CaM alone over this wavelength range, consistent with the fact the free WFF peptide is largely unstructured (Findlay et al., 1995a). The addition of excess calcium produces a major increase in intensity, with $\Delta\epsilon_M$ at 220 nm increasing by a factor of 1.39 ± 0.01 (curve c). This increase derives from two factors: the increased α-helicity of Ca_4-CaM compared with apo-CaM (Maune et al., 1992a) and the fact that the WFF peptide becomes α-helical on binding to the calmodulin (Findlay et al., 1995a). The spectrum of the apo-H2CaM (curve b) is similar to that of apo-CaM plus WFF peptide (within the

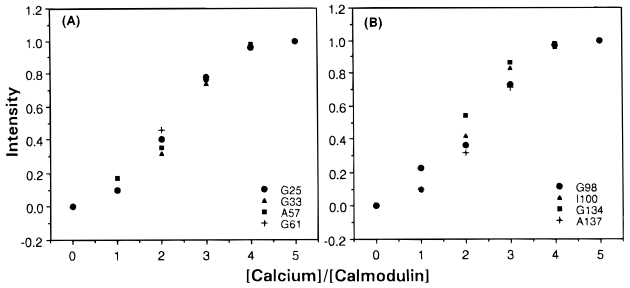

FIGURE 5: Ca^{2+} titration studies of uniformly-^{15}N-labeled H2CaM. The figure shows the peak intensity (arbitrary units) as a function of the ratio of Ca^{2+} to H2CaM. We have chosen two resonances from each EF-hand motif of the protein to show that Ca^{2+} ions fill the four Ca^{2+} sites in parallel. Panels A and B show four resonances each from the N- and C-terminal domains of the protein, respectively.

limits of the estimation of concentration). The spectrum of Ca_4-H2CaM is shown in curve d; the magnitude of the calcium-induced increase in α-helicity is very similar to that observed for CaM plus WFF peptide ($\Delta\epsilon_M$ at 220 nm increases by a factor of 1.37 ± 0.01 for the hybrid protein).

Changes in the CD intensity at 220 nm as a function of added calcium are shown in Figure 4B. For CaM plus WFF peptide, the change saturates at an R_{Ca} of 4. At $R_{Ca} = 2$, the change is some 75−80% complete. This may be contrasted with the behavior of CaM alone (Maune et al., 1992a) where the change also saturates at $R_{Ca} = 4$ but the signal increases approximately linearly with R_{Ca}. This may suggest that the peptide adopts its full α-helical structure at low values of R_{Ca} and therefore that it binds at low levels of calcium saturation. For the hybrid protein, the change at 220 nm also saturates at $R_{Ca} = 4$, but the way the signal changes as a function of R_{Ca} is very different from that seen with apo-CaM plus WFF peptide, since over 70% of the total change occurs for R_{Ca} values between 1 and 3.

Calcium Binding Studies. Changes in the ^{1}H−^{15}N HSQC spectra during a titration with calcium have been investigated. Figure 5 shows changes of the peak intensity as a function of the [calcium]/[CaM] ratio (=R_{Ca}). We have chosen two residues from each Ca^{2+} site to represent the experimental result, and it is evident that all four Ca^{2+} binding sites are filled effectively in parallel. This may be contrasted with the behavior of calmodulin alone, where the C-terminal sites are filled preferentially (Forsén et al., 1986, and references cited therein).

Typical experimental data for calcium titrations of Quin2 in the presence of apo-H2CaM or CaM plus WFF peptide are shown in Figure 6A. The values of log(K_1K_2) and log(K_3K_4) determined for *Drosophila* CaM alone agree reasonably well with values determined using the same technique with bovine testes CaM (Linse et al., 1991a) and with values determined using flow dialysis with cloned *Xenopus* CaM (Porumb, 1994) (see Table 1). Calculated curves for the variation of the degree of saturation with calcium as a function of log($[Ca]_{free}$) are shown in Figure 6B. The pCa-(50%) values calculated from the measured macroscopic binding constants are 7.75, 7.07, and 5.33 for H2CaM, CaM plus WFF peptide, and CaM, respectively.

Interestingly, the pattern of stoichiometric constants (with $K_1K_2 \gg K_3K_4$) observed with CaM alone is maintained for measurements performed in the presence of the WFF peptide. It has been argued (Linse et al., 1991a) that this pattern is

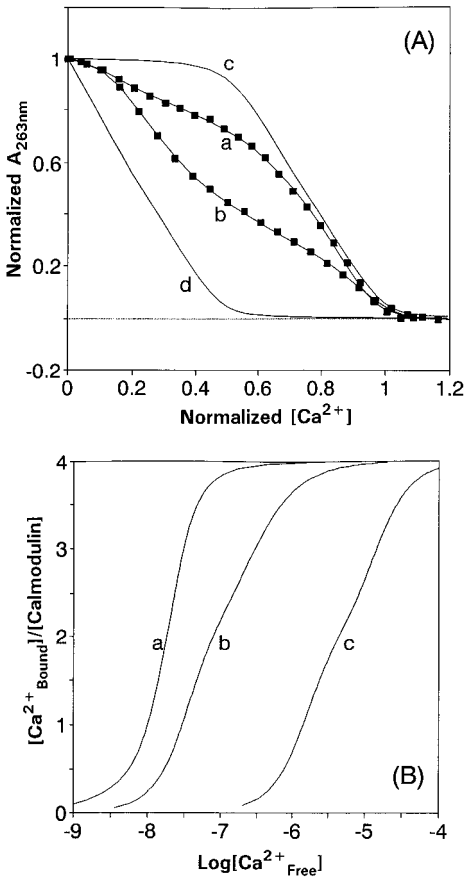

FIGURE 6: (A) Typical experimental data for calcium titrations of Quin 2 (23.9 μM) in the presence of 8.6 μM hybrid protein (curve a) and 7.4 μM calmodulin plus WFF peptide (curve b). The curves through the points are the least-squares fits to the data. Curves c and d are theoretical curves for a protein with four identical binding sites for calcium and intrinsic site binding constants of 1×10^9 M^{-1} and 1×10^3 M^{-1} (calculated for [Quin 2] = 23.9 μM and [protein] = 8.0 μM). The total calcium concentration has been normalized so that $[\text{Quin 2}]_{total} + 4[\text{protein}]_{total} = 1$. For comparison, the curves are drawn with their start and finish values at the same level. (B) Calcium binding to the hybrid protein (a), *Drosophila* calmodulin in the presence of WFF peptide (b), and *Drosophila* calmodulin alone (c). The calcium binding profiles were calculated from the stoichiometric binding constants determined from calcium titrations in the presence of Quin 2 (see Table 1).

characteristic of the situation where the C-terminal pair of calcium binding sites have much greater affinity than the N-terminal pair. The values of K_1K_2 and K_3K_4 then reflect the affinities of the C- and N-terminal Ca^{2+} ions, respectively (Linse et al., 1991a). The pattern of macroscopic binding constants for H2CaM is quite different; the values K_1K_2 and K_3K_4 are more nearly equal, suggesting that all four calcium ions bind with rather similar affinity in the hybrid protein.

The formation of the Ca_4·CaM·WFF complex may formally be represented as follows [cf. Olwin and Storm (1985)]:

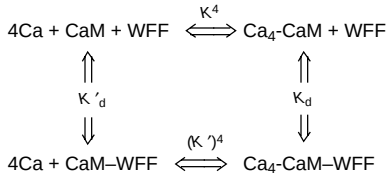

where K is the *average* affinity of a calcium ion for CaM in the absence of added WFF peptide. This is calculated as $(K_1K_2K_3K_4)^{1/4}$, where the K_i values are the measured stoichiometric *association* constants for calcium to CaM in the absence of added peptide. The value of K calculated from the measured K_i values is 2.12×10^5 M^{-1}. The constant K' is the *average* affinity of a calcium ion for CaM in the presence of added peptide. This is calculated as $(K'_1K'_2K'_3K'_4)^{1/4}$ where the K'_i values are the measured apparent stoichiometric *association* constants for calcium to CaM in the presence of added WFF peptide. The value of K' calculated from the measured K'_i values is 1.175×10^7 M^{-1}. K'_d and K_d are the *dissociation* constants for the interaction of the peptide with apo-CaM and Ca_4-CaM respectively. From Hess's Law:

$$(K')^4/K'_d = K^4/K_d \text{ and } K'_d/K_d = (K'/K)^4$$

The ratio K'_d/K_d is the factor by which the affinity of the peptide for the calmodulin is increased by the presence of calcium. For the WFF peptide, this ratio is 9.4×10^6. Since K_d is <0.2 nM (Findlay et al., 1995a), the affinity of WFF peptide for apo-CaM (K'_d) is calculated to be <1.8 mM. Values of K'_d reported in the literature cover a wide range. For example, Olwin and Storm (1985) have reported values of 80 mM and 5.7 μM for the interaction of apo-CaM with bovine heart phosphodiesterase and troponin I, respectively. For the hybrid protein, K' is 5.6×10^7 and the ratio $(K'/K)^4$ is therefore 4.85×10^9, close to 3 orders of magnitude greater than for the WFF peptide. For the hybrid protein, this thermodynamic cycle no longer applies, because the peptide is not dissociable, being covalently attached to the calmodulin. Nonetheless, this ratio gives a semiquantitative measure of the enhanced binding propensity of the tethered target sequence.

Kinetic Studies: Stopped-Flow. The addition of EGTA to Ca_4-H2CaM in the stopped-flow leads to the expected reduction in tryptophan fluorescence (see Figures 2A and 7). However, Figure 7 also shows that this change is biphasic and that the product formed in the fast phase has *more intense* fluorescence than the initial Ca_4-H2CaM complex. Similar behavior is observed in kinetic studies on the dissociation of the Ca_4-CaM−mastoparan X complex (S. E. Brown, S. R. Martin, and P. M. Bayley, unpublished observations), where it is known from calcium titrations of apo-CaM plus the peptide that the species formed at a [Ca^{2+}]/[CaM] ratio of 2 (assumed to be Ca_2-CaM−mastoparan X, in which only the C-terminal calcium sites are occupied) is *more* fluorescent than the complex Ca_4-CaM−mastoparan X. Similar results have been reported for *Polistes* mastoparan by Malencik and Anderson (1986). It is important to note here that, in contrast to the case with the mastoparans, there is no evidence for the existence of a more fluorescent intermediate in the equilibrium titration of the hybrid protein with calcium (see Figure 2C).

The observed rate constants for the fast and slow phases in the dissociation of Ca_4-H2CaM are 0.77 ± 0.05 and 0.18 ± 0.02 s^{-1}, respectively. These rates are independent of the EGTA concentration over the range 5−20 mM. The activation energies for the fast and slow phases are 65 ± 2 and 77 ± 2 kJ mol^{-1}, respectively (experiments over the temperature range 10−35 °C: data not shown).

In the case of the hybrid protein, the peptide is covalently linked to the calmodulin. It is therefore reasonable to assume that the two kinetic steps observed in the EGTA-induced

Table 1: Macroscopic Ca^{2+} Binding Constants for the CaM/M13 Hybrid Protein and for Calmodulin in the Presence and Absence of the WFF Peptide[a]

sample	log(K_1)	log(K_2)	log(K_3)	log(K_4)	log(K_1K_2)	log(K_3K_4)
Drosophila CaM	5.23 (0.14)	6.42 (0.20)	4.33 (0.31)	5.33 (0.20)	11.65 (0.15)	9.66 (0.25)
bovine CaM[b]	4.90	6.60	4.40	5.60	11.50	10.0
Xenopus CaM[c]	5.30	5.95	4.50	5.50	11.25	10.0
Drosophila CaM + WFF	6.94 (0.26)	8.01 (0.27)	6.69 (0.28)	6.64 (0.25)	14.70 (0.18)	13.33 (0.19)
CaM/M13 hybrid	7.95 (0.31)	7.45 (0.26)	7.75 (0.43)	7.84 (0.36)	15.40 (0.22)	15.59 (0.22)

[a] Measurements were made at 20 °C in 10 mM Tris, 100 mM KCl, pH 8.0. The values in parentheses are the standard deviations. [b] Determined by Linse et al. (1991a) in 2 mM Tris, 100 mM KCl, pH 7.5. [c] Determined by Porumb (1994) in 50 mM Hepes, 100 mM KCl, 1 mM $MgCl_2$, pH 7.5.

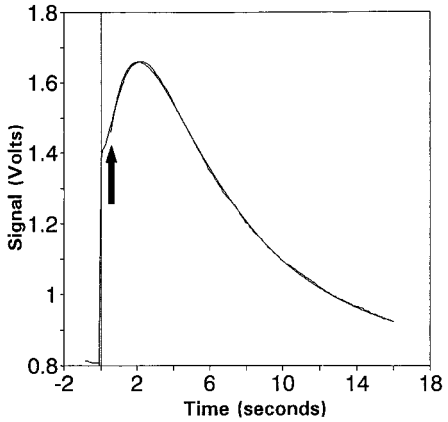

FIGURE 7: Typical stopped-flow trace for the EGTA-induced dissociation of Ca_4-H2CAM. The signal from the completely reacted solutions is ≈0.81V. The analysis started at the heavy arrow, and the fitted curve is shown superimposed on the raw data. The observed rate constants for the fast and slow phases are 0.77 ± 0.05 and 0.18 ± 0.02 s^{-1}.

dissociation correspond to the loss of the N- and C-terminal pairs of calcium ions. For the hybrid protein, these rates are seen to be similar in magnitude. Since the N-terminal pair of calcium ions dissociate more rapidly than the C-terminal pair for calmodulin in the absence of peptide (see below), we assume that for the hybrid protein the fast phase also reflects the loss of the N-terminal pair. With this mechanism, the more fluorescent intermediate would then correspond to a hybrid protein with calcium ions bound only at the C-terminal sites. We note here that the following arguments remain qualitatively the same if the fast phase corresponds to loss of the C-terminal, rather than the N-terminal, calcium pair.

For Ca_4-CaM in the absence of peptide, the dissociation rates for the N- and C-terminal calcium ions under these buffer conditions are 700 and 8.5 s^{-1}, respectively (S. E. Brown, S. R. Martin, and P. M. Bayley, in preparation). In the above mechanism for Ca_4-H2CaM, these rates are reduced by factors of 910 and 47, respectively. If the change in dissociation rate is directly related to changes in affinity for the calcium ion (i.e., if there are no changes in the association rate constants), then the ratio $(K'/K)^4$ should be equal to $910 \times 910 \times 47 \times 47 = 1.83 \times 10^9$. This agrees reasonably well with the value of 4.85×10^9 calculated in the previous section. These results also appear to confirm the deduction that the peptide portion of the hybrid protein has a significantly greater effect on the N-terminal calcium sites than it does on the C-terminal pair (a factor of 910 compared with a factor of 47), and is consistent with K_1K_2 and K_3K_4 being nearly equal for the hybrid protein. In studies on the dissociation of the Ca_4-CaM−WFF complex, we have determined a rate of 12 ± 2 s^{-1} for dissociation of the N-terminal calcium sites (S. E. Brown, S. R. Martin, and P. M. Bayley, in preparation), again confirming that there is a much greater effect on the N-terminal sites in the case of the hybrid protein.

GENERAL DISCUSSION

In this report, we have described the properties of a novel hybrid protein comprising the full length of the *Xenopus laevis* calmodulin sequence, followed by a pentapeptide linker (GGGGS) and residues 3−26 of M13, the calmodulin binding region of skeletal muscle myosin light chain kinase. Unlike the similar hybrid protein described in an earlier report (Porumb et al., 1994), the NMR evidence (Figure 1) indicates that this M13/CaM hybrid protein exists as a single conformer in solution.

A number of lines of evidence suggest that the apo-hybrid protein comprises essentially the apo-calmodulin conformation, plus the covalently attached ("tethered") peptide in a disordered conformation, with little or no specific interaction between them. Although the fluorescence emission maximum (344 nm) and the quenching characteristics both indicate that this residue is not fully accessible to the solvent, the near-UV CD of the apo-hybrid is similar to that of apo-CaM plus WFF in showing no contribution from the Trp chromophore. Also, the far-UV peptide CD of the apo-hybrid is similar to that of apo-CaM plus WFF, and the increase in intensity in this region with binding of calcium indicates an increase in helicity of the tethered peptide similar in magnitude to that of the binding of WFF to Ca_4-CaM. Hence, any interaction between the tethered peptide and the apo-CaM strucure in the apo-hybrid appears to be nonspecific in nature.

The addition of calcium to the hybrid protein produces pronounced changes in the near-UV (Figure 3B) and far-UV CD spectra (Figure 4A), in the fluorescence emission spectrum of the single tryptophan residue at position 4 in the M13 sequence (Figure 2A), and in the accessibility of this tryptophan residue to acrylamide quenching (Figure 2B). These changes are consistent with the tryptophan residue being immobilized in a hydrophobic environment and with the hybrid protein adopting a more α-helical structure when calcium is bound. The increased α-helicity derives from changes in both the calmodulin and peptide regions of the hybrid protein.

Results from $^1H-^{15}N$ HSQC NMR experiments (Figure 1) suggest that the solution structure of the calcium-saturated hybrid protein is very similar to that of the Ca_4-CaM−M13 complex (Ikura et al., 1992). Consistent with this conclusion, the optical properties (fluorescence and near- and far-UV circular dichroism) of the calcium-saturated hybrid protein

are similar to those of the complex formed between *Drosophila* calmodulin and a peptide corresponding to residues 1−18 of the M13 sequence.

Macroscopic calcium binding constants (K_1-K_4) were determined from calcium titrations performed in the presence of the calcium chelator Quin 2 (Figure 6 and Table 1). The values for $\log(K_1K_2)$ and $\log(K_3K_4)$ for *Drosophila* calmodulin alone are 11.65 ± 0.15 and 9.66 ± 0.25, respectively. As expected, the hybrid protein shows greatly increased affinity for calcium compared with calmodulin itself. The values of $\log(K_1K_2)$ and $\log(K_3K_4)$ for the hybrid protein are 15.4 ± 0.2 and 15.6 ± 0.2, respectively. The corresponding values for *Drosophila* calmodulin plus the WFF peptide are 14.7 ± 0.2 and 13.3 ± 0.2, respectively. These numbers correspond to peptide-induced increases in total calcium affinity of 9.4×10^6 for *Drosophila* calmodulin plus the WFF peptide and 4.85×10^9 for the hybrid protein. The much greater effect in the case of the hybrid protein may derive from the fact that the peptide portion is covalently linked to the calmodulin, so that the entropic cost of attaching the peptide is much reduced.

Changes in the circular dichroism (Figures 3C and 4B) and fluorescence properties (Figure 2C) of the hybrid protein as a function of the calcium to hybrid protein ratio are very different from those seen in titrations of a mixture of *Drosophila* calmodulin and the WFF peptide. The stoichiometric calcium binding constants suggest an explanation for this behavior. The situation seen with calmodulin alone (N-terminal calcium sites binding more weakly than the C-terminal ones) appears to be maintained in the presence of the WFF peptide. This may be because the 18-residue WFF peptide lacks some of the normal M13-like interactions with the N-domain of the calmodulin. A titration of apo-CaM with WFF peptide will therefore produce preferential filling of the C-terminal sites, and peptide binding to this form will produce spectroscopic changes at low levels of added calcium (see, for example, Figure 2C). With the hybrid protein, the N- and C-terminal calcium pairs appear to be much more nearly equal in affinity. This means that the presence of the covalently attached peptide portion must increase the affinity of the N-terminal sites more than that of the C-terminal ones. Stopped-flow studies provide further evidence for this interpretation. The dissociation rate for the N-terminal calcium ions is $\approx 700\ s^{-1}$ for *Drosophila* calmodulin in the absence of peptide. This is reduced to $\approx 12\ s^{-1}$ for the Ca_4-CaM−WFF complex and to less than $0.77\ s^{-1}$ for the hybrid protein.

The pattern of stoichiometric calcium binding constants observed for the hybrid protein suggested (see above) that all four calcium binding sites would fill effectively in parallel. The way the optical and NMR signals change as a function of added calcium confirms this interpretation. Figure 8 shows the fractional changes in several spectroscopic signals as a function of R_{Ca} (=[calcium]/[CaM]) for the hybrid protein. The $^1H-^{15}N$ HSQC NMR signals from residues located in the N-terminal domain (G25, G33, A57, and G61) and in the C-terminal domain (G98, I100, G134, and A137) change effectively in parallel. The tryptophan fluorescence emission intensity at 330 nm ($\lambda_{ex} = 290$ nm), the circular dichroism signals at 278 nm (calmodulin tyrosines) and 295 nm (peptide tryptophan), and the circular dichroism signal at 220 nm all change approximately in parallel with the NMR signals. Figure 8 also shows curves for the appearance of

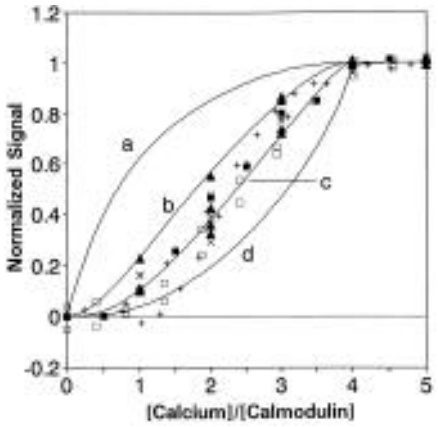

FIGURE 8: Fractional changes in various spectroscopic signals as a function of R_{Ca} (=[calcium]/[CaM]) for the hybrid protein. (+) The tryptophan fluorescence emission intensity at 330 nm (λ_{ex} = 290 nm). (□) Circular dichroism signals at 278 nm (calmodulin tyrosines) and 295 nm (peptide tryptophan). (■) Circular dichroism signal at 220 nm. (×) $^1H-^{15}N$ HSQC NMR signals from G25, G33, A57, and G61 in the N-terminal domain. (▲) $^1H-^{15}N$ HSQC NMR signals from G98, I100, G134, and A137 in the C-terminal domain. The solid lines show the appearance of different stoichiometric species calculated from the stoichiometric constants (Table 1): (a) ([Ca-H2CaM] + [Ca_2-H2CaM] + [Ca_3-H2CaM] + [Ca_4-H2CaM])/[$H2CaM_{total}$]; (b) ([Ca_2-H2CaM] + [Ca_3-H2CaM] + [Ca_4-H2CaM])/[$H2CaM_{total}$]; (c) ([Ca_3-H2CaM] + [Ca_4-H2CaM])/[$H2CaM_{total}$]; and (d) ([Ca_4-H2CaM]/[$H2CaM_{total}$].

different stoichiometric species, calculated from the macroscopic calcium binding constants. The changes in the signals associated with the interaction of the peptide portion with the calmodulin portion of the protein clearly parallel the appearance of Ca_3-H2CaM plus Ca_4-H2CaM.

The enhancement of the calcium affinity of the hybrid protein is matched by an enhanced affinity for the binding of the tethered peptide in an ordered conformation. This can be seen as a proximity or concentration effect, which avoids the large entropic energetic disadvantage of a dissociable ligand. A similar principle appears to be involved in the function of calmodulin itself as a nondissociating subunit of phosphorylase kinase, and in the reported enhanced binding of calmodulin (relative to its fragments) with smooth muscle MLCK (Persechini et al., 1994). We have recently noted the major role of the N-terminal portion of the target peptide of skeletal muscle MLCK in interacting with the C-domain of calmodulin (Findlay et al., 1995b). A general picture of the binding of calmodulin to a target protein may therefore involve a sequence of interactions starting with formation of an initial encounter complex involving a portion of calmodulin with a part of the target, and followed by completion of the full interaction by processes whose affinity and probably also kinetics are enhanced by the proximity of the remaining structural components.

The most interesting aspect of this work is that the engineered hybrid protein binds calcium with remarkably high affinity. The overall enhancement of calcium affinity by the M13 peptide analogue is 9.4×10^6, equivalent to an average increase in site affinity of 55-fold or a pCa_{50} shift of 1.74 units. In the case of the covalently linked hybrid molecule, the overall enhancement is 4.85×10^9, equivalent to an average increase in site affinity of 264-fold or a pCa_{50} shift of 2.42 units. This type of hybrid molecule is thus, in principle, capable of responding to calcium ion in the 1−10 nM concentration range. The site-directed mutagenesis

approach proposed by Beckingham and co-workers (Maune et al., 1992b) should allow us to alter the high affinity of H2CaM such that various calcium responses especially toward higher calcium concentrations can be obtained. A systematic design and characterization of such calmodulin hybrids can provide a whole new array of materials which can be used as a calcium sensor, for example, for *in vivo* studies possibly combined with fluorescent markers such as green fluorescent protein, GFP (Chalfie et al., 1994). Such a CaM hybrid fused to GFP should not perturb various CaM-dependent pathways because of the occupancy of the calmodulin target recognition site by the tethered M13 segment, and would thus be ideal for an intracellular calcium indicator. The present study on H2CaM with remarkably high affinity for calcium establishes the basis of further investigation on the design and characterization of calmodulin hybrids.

ACKNOWLEDGMENT

We thank Kit Tong and Patrick Yau for their expert help in the preparation of the hybrid protein.

REFERENCES

Babu, Y. S., Bugg, C. E., & Cook, W. J. (1988) *J. Mol. Biol. 204*, 191−204.

Barbato, G., Ikura, M., Kay, L. E., Pastor, R. W., & Bax, A. (1992) *Biochemistry 31*, 5269−5278.

Chalfie, M., Tu, Y., Euskirchen, G., Wand, W. W., & Prasher, D. C. (1994) *J. Biol. Chem. 263*, 802−805.

Davis, T. N. (1992) *Cell 71*, 557−564.

Eftink, M. R., & Ghiron, C. A. (1976) *J. Phys. Chem. 80*, 486−493.

Findlay, W. A., Martin, S. R., Beckingham, K., & Bayley, P. M. (1995a) *Biochemistry 34*, 2087−2094.

Findlay, W. A., Gradwell, M. J., & Bayley, P. M. (1995b) *Protein Sci. 4*, 2375−2382.

Finn, B. E., Evenäs, J., Drakenberg, T., Waltho, J. P., Thulin, E., & Forsén, S. (1995) *Nat. Struct. Biol. 2*, 777−783.

Forsén, S., Vogel, H. J., & Drakenberg, T. (1986) in *Calcium and Cell Function* (Cheung, W. Y., Ed.) pp 113−157, Academic Press, New York.

Gagné, S. M., Tsuda, S., Li, M. X., Chandra, M., Smillie, L. B., & Sykes, B. D. (1994) *Protein Sci. 3*, 1961−1974.

Gill, S. C., & von Hippel, P. H. (1989) *Anal. Biochem. 182*, 319−326.

Ho, S. N., Hunt, H. D., Horton, R. M., Oullen, J. K., & Pease, L. R. (1989) *Gene 77*, 51−59.

Ikura, M., Clore, G. M., Gronenborn, A. M., Zhu, G., Klee, C. B., & Bax, A. (1992) *Science 256*, 632−638.

Kay, L. E., Keifer, P., & Saarinen, T. (1992) *J. Am. Chem. Soc. 114*, 10663−10665.

Kilhoffer, M.-C., Lukas, T. J., Watterson, D. M., & Haiech, J. (1992) *Biochim. Biophys. Acta 1160*, 8−15.

Kuboniwa, H., Tjandra, N., Gresiek, S., Ren, H., Klee, C. B., & Bax, A. (1995) *Nat. Struct. Biol. 2*, 768−776.

Linse, S., Brodin, P., & Forsén, S. (1988) *Nature 335*, 651−652.

Linse, S., Helmersson, A., & Forsén, S. (1991a) *J. Biol. Chem. 266*, 8050−8054.

Linse, S., Johansson, C., Brodin, P., Grundström, T., Drakenberg, T., & Forsén, S. (1991b) *Biochemistry 30*, 154−162.

Malencik, D. A., & Anderson, S. R. (1986) *Biochem. Biophys. Res. Commun. 135*, 1050−1057.

Martin, S. R., & Bayley, P. M. (1986) *Biochem. J. 238*, 485−490.

Martin, S. R., Andersson Teleman, A., Bayley, P. M., Drakenberg, T., & Forsén, S. (1985) *Eur. J. Biochem. 151*, 543−550.

Maulet, Y., & Cox, J. A. (1983) *Biochemistry 22*, 5680−5686.

Maune, J. F., Beckingham, K., Martin, S. R., & Bayley, P. M. (1992a) *Biochemistry 31*, 7779−7786.

Maune, J. F., Klee, C. B., & Beckingham, K. (1992b) *J. Biol. Chem. 267*, 5286−5295.

Meador, W. E., Means, A. R., & Quiocho, F. A. (1992) *Science 257*, 1251−1255.

Olwin, B. B., & Storm, D. R. (1985) *Biochemistry 24*, 8081−8086.

Persechini, A., McMillan, K., & Leakey, P. (1994) *J. Biol. Chem. 269*, 16148−16154.

Porumb, T. (1994) *Anal. Biochem. 220*, 227−234.

Porumb, T., Yau, P., Harvey, T. S., & Ikura, M. (1994) *Protein Eng. 7*, 109−115.

Thulin, E., Andersson, A., Drakenberg, T., Forsén, S., & Vogel, H. J. (1984) *Biochemistry 23*, 1862−1870.

Tjandra, N., Kuboniwa, H., Ren, H., & Bax, A. (1995) *Eur. J. Biochem. 230*, 1014−1024.

Török, K., Lane, A. N., Martin, S. R., Janot, J.-M., & Bayley, P. M. (1992) *Biochemistry 31*, 3452−3462.

Urbauer, J. L., Short, J. H., Dow, L. K., & Wand, A. J. (1995) *Biochemistry 34*, 8099−8109.

Waltersson, Y., Linse, S., Brodin, P., & Grundström, T. (1993) *Biochemistry 32*, 7866−7871.

Yagi, K., Yazawa, M., Ikura, M., & Hikichi, K. (1989) in *Calcium Protein Signalling* (Hidaka, H., Carafoli, E., Means, A. R., & Tanaka, T., Eds.) pp 147−154, Plenum Publishing Co., New York.

Yazawa, M., Ikura, M., Hikichi, K., Luan, Y., & Yagi, K. (1987) *J. Biol. Chem. 262*, 10951−10954.

Yazawa, M., Vorherr, T., James, P., Carafoli, E., & Yagi, K. (1992) *Biochemistry 31*, 3171−3176.

Zhang, M., Tanaka, T., & Ikura, M. (1995) *Nat. Struct. Biol. 2*, 758−767.

BI952522A